Inter-Research Science Publisher

Endangered Species Research
Volume 57:325–340

Published August 14, 2025
https://doi.org/10.3354/esr01423

Accounting for sampling bias reveals a decline in abundance of endangered false killer whales in the main Hawaiian Islands

Janelle J. Badger[1,*], Robin W. Baird[2], Devin S. Johnson[1], Amanda L. Bradford[1], Sabre D. Mahaffy[2], Michaela A. Kratofil[2,3,4], Tori Cullins[5], Jens J. Currie[6], Stephanie H. Stack[7], Erin M. Oleson[1]

[1]Pacific Islands Fisheries Science Center, NMFS, NOAA, 1845 Wasp Boulevard, Building 176, Honolulu, HI 96818, USA

[2]Cascadia Research Collective, 218½ West 4th Avenue, Olympia, WA 98501, USA

[3]Marine Mammal Institute, Oregon State University, 2030 SE Marine Science Dr, Newport, OR 97365, USA

[4]Department of Fisheries, Wildlife, and Conservation Sciences, Oregon State University, 2820 Campus Way, Corvallis, OR 97331, USA

[5]Wild Dolphin Foundation, 87-1002 C Hakimo Place, Waianae, HI 96792, USA

[6]Pacific Whale Foundation, 300 Maʻalaea Road, Suite 211, Wailuku, HI 96793, USA

[7]Southern Ocean Persistent Organic Pollutants Program, School of Environment and Science, Griffith University, Nathan, QLD 4111, Australia

ABSTRACT: We estimated abundance of the endangered main Hawaiian Islands (MHI) insular population of false killer whales *Pseudorca crassidens* from 1999–2022 using a modeling technique that incorporates animal availability in a capture–recapture analysis. The population was sampled using different sampling methods, resulting in yearly encounter histories of 265 individuals and 53 satellite-tagged whales. Survey effort and animal location data were separately analyzed using kernel density estimators, and the degree of overlap between these 2 processes was used to model detection probability in a Bayesian Jolly-Seber population model. This approach better addresses spatiotemporally variable sampling effort than traditional capture–recapture methods, improving the estimation of reliable abundance trends. Using simulated data, the model was robust to many sampling and ecological complications, such as variable low detectability, unequal tag deployment lengths, and variable social group sizes. Fitting the model to the MHI false killer whale data set, we found that the insular population of false killer whales remains small, with an estimated 139 individuals (95% credible interval, CRI = [114, 162]) in 2022. The population appears to be in decline throughout the study period, with a mean annual percent change of −1.09 (95% CRI = [−2.11, −0.023]) over the entire time series and −3.51 (95% CRI = [−5.08, −1.88]) since 2013, when the population was listed as endangered. Given the magnitude of the decline, identifying which of the many factors affecting this population is most responsible is key in order to guide potential management responses.

KEY WORDS: Telemetry · Data integration · Mark–recapture · Endangered species · Jolly-Seber · False killer whales

HŌʻULUʻULU MANAʻO: Koho mākou i ka nui o nā pūʻuo ʻanehalapohe o nā koholā ʻāhuka iwi poʻo like (*Pseudorca crassidens*) a puni ka paeʻāina ʻo Hawaiʻi (MHI) mai nā makahiki 1999-2022 ma o kekahi ʻōnaehana e kālailai ana i ka loaʻa ʻana o ka holoholona i kekahi kālailai loaʻa-loaʻa hou. Mai nā makahiki 1999-2022 mai, he mau kiʻina ʻohi hāpana i nānā ʻia a ʻo ka loaʻa, ʻike kūmakahiki ʻia he 265 koholā iwi poʻo like a he 53 mea i poelele lepili ʻia. Kālailai pākahi ʻia ke anapūʻuo a me ka ʻikepili henua ma o nā koho paʻapū kenele, a ʻo ka nui o ke kaulapa ma waena o ia mau ʻelua, ua hoʻohana ʻia

*Corresponding author: janelle.badger@noaa.gov

Publisher: Inter-Research · www.int-res.com

i kumu ho'ohālike i ka papaha 'ikena ma ka pū'uo ho'ohālike Bayesian Jolly-Sever. 'Oi aku ka maika'i o kēia hana ma mua o nā hana loa'a-loa'a hou ma'amau no ka nānā 'ana i nā 'ano ao henua 'ohi hāpana, a he ho'oikaika i ke koho i ka 'aui 'ana o nā lawa kūpono. Ma ka ho'ohana 'ana i ka 'ikepili ho'okūkohukohu 'ia, he kumu ho'ohālike maika'i nō kēia i ka nui 'ohi hāpana a me ka nui o nā hopena kaiaola, e la'a ho'i me ke kumuloli 'ikena ha'aha'a, ka lō'ihi o ka lepili 'oko'a, a me ke kumuloli o ka nui pū'ulu launa. Ma ka launa 'ana o ia kumu ho'ohālike me ka 'ikepili o ko Hawai'i pae'āina koholā 'āhuka iwi po'o like, 'ike mākou i ka li'ili'i mau o ka pū'uo koholā 'āhuka iwi po'o like 'ane'ane puni 'ia e ke kai, ma kahi o 139 (95% CRI = [114, 162]) ma ka makahiki 2022. Ma o ka wā kālailai, kohu mea lā, emi mai ka pū'uo, he -1.09 pākēneka loli (95% CRI = [-2.11, -0.023]) 'awelike o ka makahiki, a he -3.51 (95% CRI = [-5.08, -1.88]) mai ka makahiki 2013, i ka wā i helu 'ia ai ka pū'uo he mea 'anehalapohe. No ka nui o ia 'ano emi 'ana, ko'iko'i nō ka 'ike 'ana i nā mea e pā nui ana i kēia pū'uo i mea e alaka'i aku ai i nā hāpane ho'oponopono.

1. INTRODUCTION

The importance of detecting declines in wildlife populations has long been recognized (Ceballos & Ehrlich 2002). Even in cases where species extinction is not imminent, population decline can lead to localized extirpation and loss of ecosystem function and services (Ceballos & Ehrlich 2002, Nichols & Williams 2006). Identifying that population declines are occurring and the factors that may be driving losses of individuals is needed to inform conservation and management planning. Detecting trends in population growth, positive or negative, allows for an evaluation of the efficacy of management actions and can inform future decision-making (Yoccoz et al. 2001). However, the challenges of data collection, particularly for dispersed or inaccessible species such as marine mammals, can lead to time series of abundance or related indices that lack the statistical power to detect declines (e.g. Taylor et al. 2007). This predicament emphasizes the importance of incorporating novel analytical techniques and auxiliary data sets in what may otherwise be considered the best available science (e.g. Murphy & Weiland 2016) when assessing marine mammal and other difficult-to-study wildlife populations.

False killer whales *Pseudorca crassidens* are an example of a species whose life history and behavior makes them challenging to survey and, consequently, collect data necessary for robust evaluation of their population dynamics. False killer whales are long-lived (females live well into their 60s) and are slow to mature (10–15 yr old at sexual maturity; Ferreira et al. 2014, Photopoulou et al. 2017). They are strongly social, known to often travel in large, coordinated groups, and exhibit cohesive social structure (Baird et al. 2008, Mahaffy et al. 2023). They have a matrilineal social structure, with strong, long-term bonds, and they are one of a few species where females are known to undergo a post-reproductive period (Photopoulou et al. 2017, Martien et al. 2019). False killer whales inhabit sub-tropical and tropical oceanic regions worldwide (Stacey et al. 1994, Baird 2018, Zaeschmar & Estrela 2020), and a number of coastal and island-associated populations have been documented (Baird et al. 2008, Silva et al. 2013, Zaeschmar et al. 2014, Baird 2016, Palmer et al. 2017, Douglas et al. 2023). Their generally offshore distribution and tendency to move frequently over large spatial domains (Baird et al. 2012, Anderson et al. 2020) make it challenging to adequately survey their populations.

The main Hawaiian Islands (MHI) insular population of false killer whales is small, last estimated to number 167 ± 23 individuals in 2015 (Bradford et al. 2018). This population is sparse throughout their range, with individuals known to move widely among and frequently between island areas within the MHI (Baird et al. 2012). Individuals preferentially form social groups, hereafter referred to as 'clusters' (Mahaffy et al. 2023). Four stable clusters have been recognized (Mahaffy et al. 2023) that consist of family members and regular associates (Martien et al. 2019). There has been some evidence for cluster-specific space-use patterns (Baird et al. 2012, 2023, Mahaffy et al. 2023). When encountered during survey effort, individuals and subgroups within larger groups are often spread out, traveling 10s of km apart (Bradford et al. 2014, Baird 2016). The MHI insular population of false killer whales was listed as endangered under the US Endangered Species Act in 2012 following a decline in recent decades (Oleson et al. 2010). The greatest suspected threats to this population's viability include interactions with nearshore fisheries (Baird et al. 2015), exposure to pollutants (Ylitalo et al. 2009, Bachman et al. 2014, Kratofil et al. 2020), and reduced genetic diversity (Chivers et al. 2010, Martien et al. 2014).

The MHI insular population is the most thoroughly studied population of false killer whales in the world, with numerous boat-based surveys, photo-

identification, satellite-telemetry, and genetic studies conducted over the last few decades (Baird 2016). Individually, each of these data streams presents unique challenges to estimate crucial metrics (such as abundance and population growth rate) to monitor this endangered population. For example, there is variable boat-based survey effort around the MHI, and as this population is wide-ranging, these surveys will only encompass a small proportion of the population's range in any given period. Weather and sea conditions generally further restrict areas viable for visual sampling, with surveys almost exclusively conducted on leeward sides of islands protected from trade winds (Baird et al. 2013, 2024). Without information on individual space use (e.g. if animal movement is random with respect to island geography), it is unclear how this sampling may affect capture availability and subsequent metrics.

Substantial work has been done to estimate abundance for this population through photo-identification-based capture–recapture (CR) models, generating estimates that are robust to many forms of sampling variability and bias (Bradford et al. 2018). However, availability bias is inadequately accounted for within conventional CR models (Marsh & Sinclair 1989, Hammond et al. 2021). Abundance estimates resulting from conventional CR models only represent the sampled population in each year rather than the annual full population abundance. As it is unclear what proportion of the MHI false killer whale population is sampled each year, the estimates obtained by Bradford et al. (2018) were insufficient to determine population trend, and thus difficult to incorporate into recovery plans.

Here, we estimate yearly abundance and long-term trend of the MHI insular population of false killer whales from 1999 to 2022 using a novel CR modeling technique that incorporates animal space use information to more fully alleviate sampling bias concerns (detailed in Badger et al. 2024). Our results provide a more robust estimate of yearly abundance and recent population trends, allowing an examination of this population's dynamics since it was listed as endangered.

2. MATERIALS AND METHODS

2.1. Data collection

Data used in this analysis were predominantly sourced from dedicated nonrandom, nonsystematic small-boat surveys for odontocetes conducted by Cascadia Research Collective (CRC) from 1999 to 2022 (Fig. 1). Collectively, CRC has conducted surveys of nearshore waters around all MHI; however, only a few areas can be surveyed every year and more than half of the effort has been undertaken off of Hawai'i Island (Baird et al. 2024). Generally, 1–6 occasions of such efforts lasting 1–6 wk were conducted throughout each year. Areas selected to be surveyed are designed to maximize the probability of animal encounters (details of the field operations are provided in Baird et al. 2013, 2024). Even with this focused sampling, false killer whales are only rarely encountered, with just 124 group sightings from 1999 to 2022, making up 3.8% of all odontocete sightings (Baird et al. 2024). At each false killer whale group sighting, researchers recorded the location of the group and took photographs for individual identification based on the prevalence of persistent markings (e.g. nicks, notches) on the leading and trailing edge of the dorsal fin (Baird et al. 2008). Individuals considered 'distinctive' or 'very distinctive' (Baird et al. 2008), hereafter characterized as 'distinctive', were assigned to 1 of 4 identified social clusters using the analysis of network modularity explained in Mahaffy et al. (2023).

Along with their own archive, CRC has curated photos from other research groups, such as NOAA Fisheries Pacific Islands Fisheries Science Center (PIFSC), the Pacific Whale Foundation (PWF), and Wild Dolphin Foundation (WDF) as well as from ocean users such as whale watch operators and photographers (Fig. 1). High-quality photographs of distinctive individuals from all relevant sources were combined following Bradford et al. (2018). Encounter data were then compiled at the annual scale, with distinctive individuals recorded as either encountered or not encountered each year.

When crew expertise, ocean conditions, and animal behavior allowed, CRC and PIFSC research efforts also included satellite tag deployments to obtain information on false killer whale space use (see Baird et al. 2010). Between 2007 and 2022, whales were tagged using location-only satellite tags (SPOT5 or SPOT6; Wildlife Computers), or location-and-dive behavior-transmitting satellite tags (SPLASH10 or SPLASH10-F Fastloc®-GPS; Wildlife Computers) in the low-impact minimally percutaneous external-electronics transmitter (LIMPET) configuration (Andrews et al. 2008). Relevant permits for tagging were issued by NOAA Fisheries, and the methods were approved by the Institutional Animal Care and Use Committees of CRC and PIFSC. The tags were deployed with a pneumatic projector and attached using two 6.7 cm

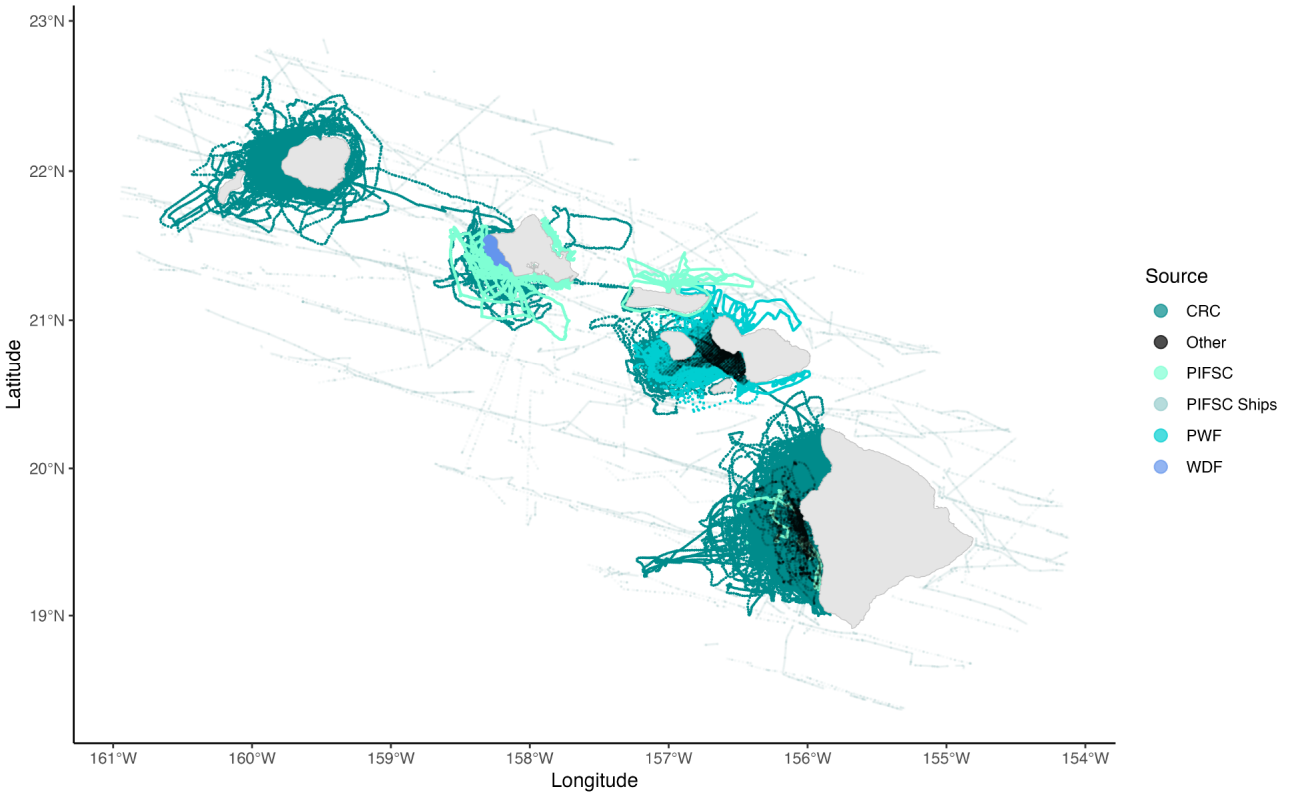

Fig. 1. Tracks from cetacean surveys conducted by Cascadia Research Collective (CRC), Pacific Islands Fisheries Science Center (PIFSC, with systematic ship surveys in light grey), Pacific Whale Foundation (PWF), and Wild Dolphin Foundation (WDF), as well as other opportunistic contributors, from 1999 to 2022 in the main Hawaiian Islands. The extent of the mapped tracklines represents the boundary of the main Hawaiian Islands insular false killer whale population (Bradford et al. 2015)

surgical-grade titanium darts with backward-facing petals to the dorsal fin (or just below the fin) of the whales. Tag duty cycles were configured to transmit during hours with the greatest probability of a satellite pass occurring in the study area.

Prior to analyses, location data were filtered through the Douglas-Argos Filter (Douglas et al. 2012) via Movebank (Kranstauber et al. 2011) to filter out locations based on unrealistic traveling speeds and turning angles (see Baird et al. 2012 for user-defined settings). Fastloc®-GPS locations for relevant tag deployments (n = 2) were filtered by first excluding locations with residual values greater than 35 and time errors greater than 10 s (Dujon et al. 2014). Resulting GPS locations were then processed through a general speed filter via Movebank (Kranstauber et al. 2011). When tags were deployed on multiple individuals from the same group, one of each pair of tagged individuals moving in concert was removed before analyses to avoid pseudoreplication, allowing tagged individuals to represent their respective group (see Schorr et al. 2010 for details).

2.2. Statistical analysis

To account for the spatiotemporal variability in sampled areas, we used a novel pseudospatial technique following Badger et al. (2024). This method involves estimating the coverage of survey effort relative to animal space use, hereafter referred to as 'overlap', and using this variable to inform animal availability within a CR model. The multistep process entails (1) computing a kernel density estimate of individual tagged whales and scaling to social clusters to estimate population-level 'animal space use'; (2) computing kernel density estimates of survey effort from research groups and ocean users to obtain estimates of 'survey coverage'; (3) determining availability of animals to survey coverage by finding the interaction between (1) and (2), or the overlap, using Bhattacharyya's affinity (BA); and (4) incorporating this overlap measure within the detection process of an open-population Jolly-Seber CR model (Jolly 1965, Seber 1965) fit in a Bayesian framework.

2.2.1. Describing animal space use

As described in Badger et al. (2024), first, for each tagged false killer whale, locations were fit to a continuous-time correlated random walk (CTCRW) model using the R (v.4.2.2; R Core Team 2022) package 'crawl' (v.2.2.1; Johnson et al. 2008) to account for location error and predict locations (paths) from observed animal locations. These imputed paths were then rerouted around islands using the R package 'pathroutR' (London 2020). Then, individual utilization distributions (UDs) were described by a kernel density estimator (KDE) using the R package 'ks' (Duong 2007). For the KDE, we used a plug-in bandwidth (h_i) equal to:

$$h_i = n_{ei}^{-1/3} \cdot \mathbf{\Sigma_i} \quad (1)$$

where $\mathbf{\Sigma_i}$ is the covariance matrix among locations for the i^{th} individual and n_{ei} is the effective sample size (ESS), as described by Gelman et al. (2013) and updated in Vehtari et al. (2021), of the i^{th} telemetry data set. The ESS uses the correlation structure of the CTCRW model to assess the effective number of observations that will be less than the total number of observed locations, which will inflate the kernel size. This approach seeks to produce a more predictive UD that accounts for the limited time observation of an animal's correlated travel, similar in effect to the autocorrelated KDE (AKDE, Fleming et al. 2015). The full form of the KDE for the i^{th} tagged individual, $\hat{f}_i$, is given below.

Let $s = (s_1,...,s_n)$ be tag locations, such that $s_j = \{x_j, y_j\}$, where $j \in \{1,...,n_i\}$ and n_i is the total number of locations for the i^{th} individual. Then,

$$\hat{f}_i(s) = \frac{1}{n_i \cdot h_i} \sum_{j=1}^{n_i} K\left(\frac{s - s_j}{h_i}\right) \quad (2)$$

where K is a Gaussian kernel, i.e. $K(u) = \frac{1}{\sqrt{2\pi}} e^{-\frac{1}{2}u^2}$. The resulting $\hat{f}_i$ was then normalized to sum to 1 over the study area.

The resulting UD provided a density surface for individual presence in space. However, in order to use the tag data information for animals not equipped with telemetry tags in the CR sample, we required an estimate of population-level space use to determine animal availability during our survey efforts. While there are many ways to weight individual UDs when averaging (see Conn et al. 2022), we aimed to develop an overall use index for use as a covariate in a CR model that can be adjusted to best model detections using the associated coefficients of the model. Therefore, we used the straight average UD. Given that this population is known to be affiliated as stable, distinct social clusters, these individual UDs were summed by social cluster to a 'cluster UD', henceforth referred to as UD_c, where $c \in \{1,2,3,4\}$ for the current 4 cluster designations (Fig. 2).

2.2.2. Defining survey effort

Survey effort for the purpose of this analysis was computed using time-specific kernel density estimates based on contributor coverage of the waters around the MHI. CRC's surveys were nonsystematic and nonrandom, although they did attempt to cover a broad range of habitats and space over the course of each sampling period. Alternatively, PWF generally used a systematic approach, and other ocean users opportunistically encountered false killer whales on routine whale- or dolphin-watching tours or fishing routes. PIFSC encountered false killer whales while on systematic ship-based surveys, such as the Hawaiian Islands Cetacean and Ecosystem Assessment Survey (Yano et al. 2018), as well as on nonsystematic and nonrandom ship and small-boat surveys.

As each contributor to the photo-identification archive used varying methods to encounter false killer whales throughout the study, we used a flexible approach to defining effort. For the 3 largest contributors to the archive (CRC, PWF, and PIFSC), survey tracks were recorded via an affixed GPS for almost the entire time series (details of the field operations for PWF are provided in Stack et al. 2019). WDF, another main contributor, provided GPS tracks when available, but these were not recorded for many years. WDF, along with other organizations and other contributing ocean users, were able to define regularly covered areas that for many of these sources, were visited daily throughout the year. We randomly sampled 1000 points within these defined effort areas (using R package 'sf'; Pebesma 2018) for inclusion in the KDE for each year the contributor was active. Photographs from individuals or groups that did not provide any effort information were not included in this analysis, although these photos accounted for only a very small proportion of the total yearly records (~3.6%).

We computed survey effort coverage using a simple KDE of survey tracks and sampled points from effort areas e for each year t, subsequently referred to as $UD_{e,t}$ for $t \in \{1,...,T\}$, where T is the data time series length, and with a bandwidth based on a reasonable maximum sighting distance from the survey vessels (2 km on each side). Although this seems like a large maximum detection distance, false killer whales are a

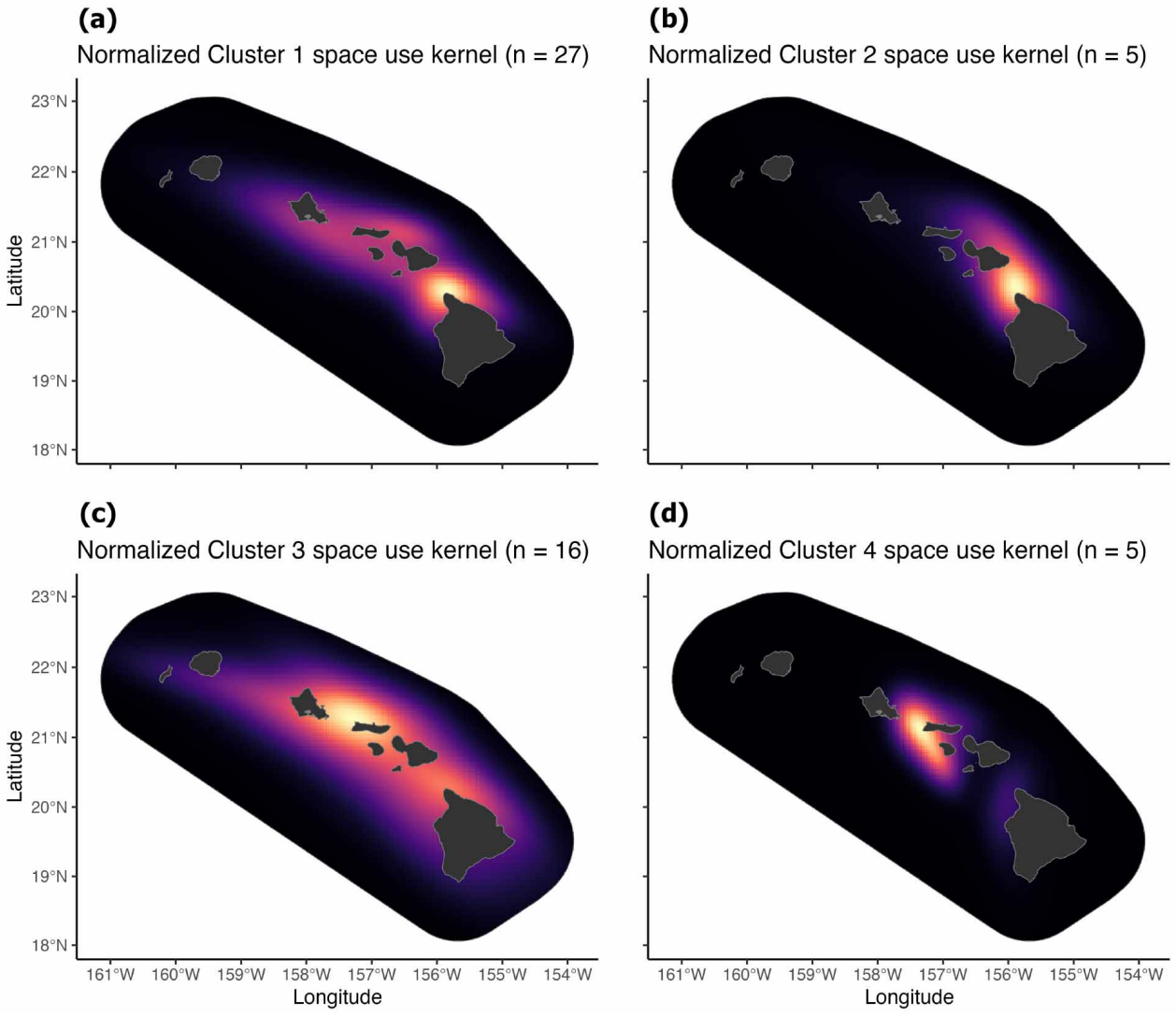

Fig. 2. (a–d) Cluster-level space use of main Hawaiian Islands insular false killer whales determined from kernel density estimators of location data from 53 satellite-tagged groups from 4 social clusters from 2007 to 2022. The extent of the mapped area represents the boundary of the main Hawaiian Islands insular false killer whale population (Bradford et al. 2015)

highly surface-active species that are typically only surveyed during ideal weather conditions.

2.2.3. Computing the overlap metric

To calculate the overlap between animal space use, UD_c, and survey efforts, $UD_{e,t}$, we computed BA:

$$BA_{c,e,t} = \int_x \int_y \sqrt{UD_c(x,y)} \cdot \sqrt{UD_{e,t}(x,y)} \quad (3)$$

where $UD_c(x,y)$ and $UD_{e,t}(x,y)$ are the values of the UD of the clusters and survey efforts, respectively, at the point (x,y) in the year t, where $t \in \{1,...,T\}$. This overlap measure was then standardized over time for modeling purposes, i.e.:

$$Overlap_{c,t} = \frac{BA_{c,e,t} - \mu}{\sigma}$$

where

$$\mu = \frac{1}{T}\sum_1^T BA_{c,e,t} \text{ and } \sigma = \sqrt{\frac{\Sigma (BA_{c,e,t} - \mu)^2}{T}} \quad (4)$$

2.2.4. Model form

We used the overlap variable as a covariate in the detection process of a hierarchical Jolly-Seber open-population CR model to estimate abundance (Jolly 1965, Seber 1965, also see Kéry & Schaub 2012). As described in Badger et al. (2024), at each sampling occasion (in this case, year), individuals

can be in 1 of 3 possible states: 'not yet entered', 'alive', or 'dead', and transitions among these states are governed by 2 ecological processes: entry and survival.

Suppose we have an augmented population of M individuals, of which N are genuine and $M - N$ are pseudo-individuals. Entry is described using ψ, the probability that governs movement from the state 'not yet entered' (i.e. appended animals not entered in the population of interest yet) to the state 'alive'. The state of individual i at the first occasion is determined by a Bernoulli trial with probability ψ at the first time step:

$$z_{i,1} \sim \text{Bernoulli}(\Psi_1) \tag{5}$$

Subsequent states are determined either by survival, ϕ, for an individual already entered ($z_{i,t} = 2$) or by entry, Ψ_t, for those that have not ($z_{i,t} = 1$) via a transition matrix:

$$z_{i,t} \mid z_{i,t-1} \sim \begin{array}{c} \\ \text{not yet entered} \\ \text{alive} \\ \text{dead} \end{array} \begin{array}{c} \begin{array}{ccc} \text{not yet entered} & \text{alive} & \text{dead} \end{array} \\ \begin{pmatrix} 1-\psi_t & 0 & 0 \\ \psi_t & \phi_t & 0 \\ 0 & 1-\phi_t & 1 \end{pmatrix} \end{array} \tag{6}$$

Similarly, observations are governed by a detection process with detection probability p, that depends on an individual's cluster assignment, c_i:

$$y_{i,t} \mid z_{i,t} \sim \begin{array}{c} \\ \text{observed} \\ \text{unobserved} \end{array} \begin{array}{c} \begin{array}{ccc} \text{not yet entered} & \text{alive} & \text{dead} \end{array} \\ \begin{pmatrix} 0 & p_{i,t} & 0 \\ 1 & 1-p_{i,t} & 1 \end{pmatrix} \end{array} \tag{7}$$

where $\text{logit}(p_{i,t}) = \alpha_t + \delta \times \text{overlap}_{ci,t}$, with estimated parameter intercepts α_t and coefficient for overlap δ.

Population abundance in a given year, N_t, is then defined as the number of distinctive individuals in the 'alive' state; that is, $N_t = \Sigma_i \text{I}(z_{i,t} - 2)$, where $\text{I}(x)$ is an indicator that $x = 0$.

We fit a saturated model, with time-varying detection, entry, and survival. To ease model fit and identifiability, we set the mean detection of the first 2 occasions equal ($\alpha_1 = \alpha_2$) and used a smoothed function (penalized regression splines) of survival. To achieve the smooth function, in pre-processing we simulated binomial draws based on the previously estimated constant annual survival rate (0.94; Bradford et al. 2018), fit a generalized additive model (GAM) using the R package 'mgcv' (Wood 2011), and extracted the values of the linear predictor, coefficients, and variance–covariance matrix from the model fit as the prior for the sequence of survival estimates.

2.2.5. Accounting for nondistinctive individuals

Importantly, in using photo-identification for CR analyses, abundance estimates N_t will only reflect the number of distinctive individuals in the population, as nondistinctive individuals are excluded from our data set (until they become distinctive; Hammond et al. 1990). To estimate total abundance, we must adjust abundance estimates by the proportion of the population that is distinctive in each year (θ_t). Total abundance is then estimated by the Horvitz-Thompson ratio $N_{\text{total},t} = N_t / \theta_t$, where $N_{\text{total},t}$ is the abundance of all individuals (distinctive and nondistinctive) at each capture occasion t.

We estimated θ_t in pre-processing using photographs taken from encounters by CRC where the number of nondistinctive and distinctive individuals were determined in each encountered group to estimate the proportion of distinctive individuals in the population in each year, expanding on the approach of Bradford et al. (2018) by accounting for variation through time and including all observed groups regardless of size. We fit a binomial (logit link) GAM to these data using the R package 'mgcv' (Wood 2011) with year as a covariate to obtain a smoothed function of the proportion of distinctive individuals by year. We then extracted the values of the linear predictor, coefficients, and variance–covariance matrix to generate a prior on the time series of θ_t. At each iteration of the CR Markov chain Monte Carlo (MCMC; see details in Section 2.2.8), we pulled predicted curves from this model (Fig. 3) to appropriately propagate uncertainty in θ_t to the $N_{\text{total},t}$ calculation that adjusted our abundance estimates to account for nondistinctive individuals in the population. For CRC encounters, efforts were consistently made to photograph all individuals in each group, regardless of distinctiveness. Given that CRC encounters comprise the majority of this data set, we deemed it reasonable to apply estimates of θ from CRC encounters to those from all contributors.

2.2.6. Trend estimation

To determine the trend in abundance for this population, we regressed the series of generated total population sizes $N_{\text{total},t}$ against time for each iteration of the MCMC, estimating a population trend as the slope parameter of the regression model that quantifies the change in abundance over time. This method results in a posterior distribution of trends that translates the uncertainty in these abundance estimates to

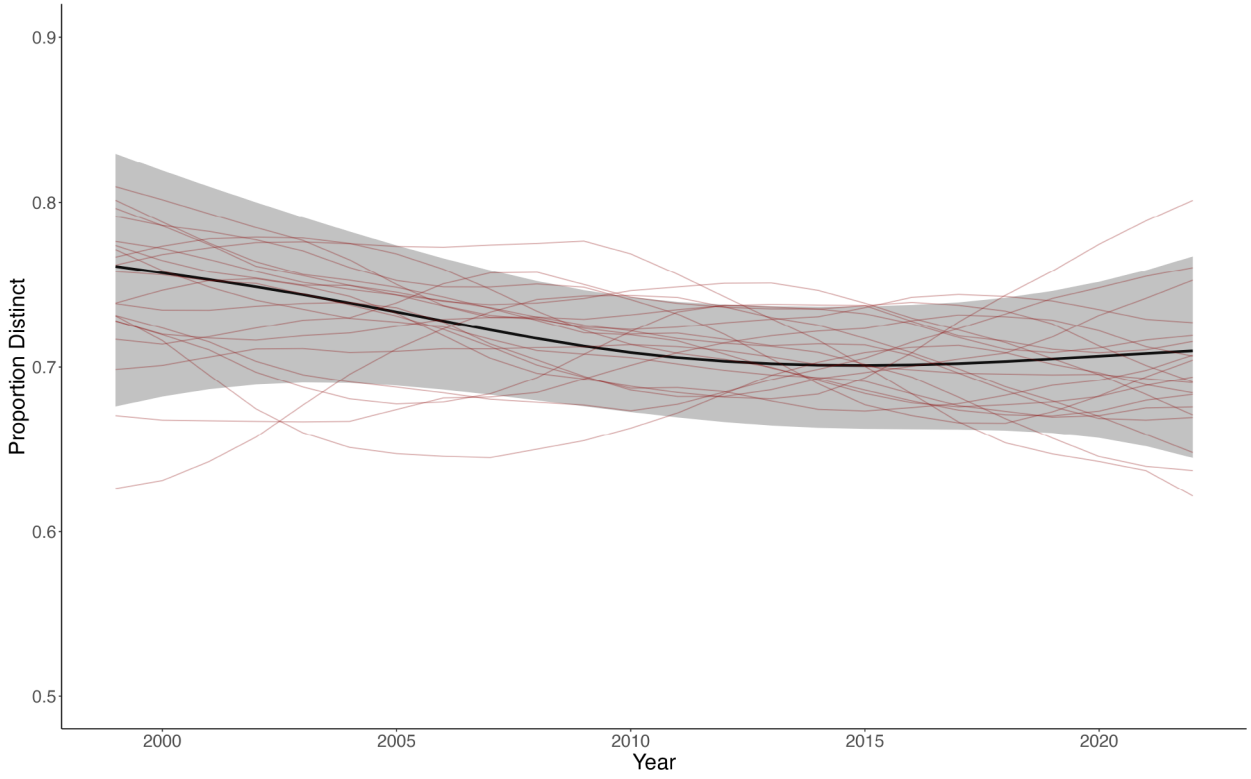

Fig. 3. Output of generalized additive model fit to the proportion of distinctive individuals in sightings of main Hawaiian Islands insular false killer whales by the Cascadia Research Collective from 1999 to 2022. Black line and grey shaded area: mean and 95% confidence interval of the predicted relationship between proportion distinctive and year. Red lines: sample draws of the multivariate normal distribution estimated by the model output, which comprised the prior distribution used for proportion distinctive in the capture–recapture Markov Chain Monte Carlo

necessary uncertainty in population trend. As another method to present population trend, we calculated the annual percent change in abundance estimates at each iteration of the MCMC.

2.2.7. Simulations of model performance

Simulations of this model's performance under varying conditions were conducted in Badger et al. (2024) and showed that it was robust to many realistic complications, such as variable cluster-level space use and low detectability. Upon fitting the pseudospatial model to the full false killer whale data set, we conducted further simulations to examine how the performance of this model is affected by some of the complications arising in our system, such as variable tag deployment durations, population trends, and variable cluster abundances. Following the procedure in Badger et al. (2024), we simulated animal movements, survey efforts, and resulting capture histories of 300 individuals comprising 3 clusters. Starting locations for group-level movements and survey effort were chosen at random at each of 10 time steps, and subsequent movement and survey tracks were modeled as correlated random walks (using package 'adehabitatLT' v.0.3.26; Calenge 2006). For each of the 10 time steps, surveys would detect individuals with a detection probability of 0.2 if they were <2 km from the survey vessel. The resulting capture histories were then fit to a pseudospatial Jolly-Seber model outlined above in a Bayesian framework. Six simulated individuals from each cluster were telemetered, and their locations were used to estimate the cluster-level UDs for which survey overlap was determined.

Tag deployment durations were either equal among tags, at a mean of 62.86 d, or were pulled from a normal distribution with parameters $\mu = 62.86$ d and $\sigma^2 = 48.23$ truncated to >0, the sample mean and standard deviation derived from available telemetry data. We also simulated positive and negative trends in abundance, with the slope of abundance over the time series as −5 or +5 individuals per annum. As we also want to ensure the pseudospatial model did not perform poorly relative to the conventional CR model in conditions with variable population trajectories, we

also compared our model to a conventional model in altering trends. Cluster abundances were either equal, with 100 individuals in each group, or unequal, distributed as 50, 100, and 150 individuals.

As described in Badger et al. (2024), this procedure was repeated 30 times per set of conditions (equal vs. unequal cluster abundances, equal vs. unequal tag deployment durations, positive vs. negative population trends) to observe the range of probabilistic outcomes in capture histories. For each model, we report the difference in posterior precision, the number of inaccurate abundance estimates (see below), and the proportion of simulated data sets whose abundance estimates exhibit an inaccurate trend. We define an inaccurate abundance estimate as one where the 90% credible interval (CRI) of the posterior distribution did not contain the true population size. To detect inaccurate trends, at each iteration of the Bayesian MCMC, we regressed derived abundance estimates over time and defined an inaccurate trend if the 90% CRI of the resulting slope parameter posterior distribution was distinct from the simulated trend (−5, 0, or +5).

2.2.8. Model fitting and selection

The pseudospatial CR model, as well as a null model without the overlap variable, was fit to the annual encounter histories compiled for each relevant individual in the photo-identification data set. For further exploration of model formulations of a conventional Jolly-Seber model fit to a previous version of this data set, see Bradford et al. (2018). A Bayesian framework was used for model fitting, selection, and inference using the software JAGS (v.4.2.0) through the R interface 'rjags' (Plummer 2003, 2018). We used an informative Beta(8,2) prior for survival rate ϕ (given the longevity of false killer whales), but otherwise uninformative priors, namely Uniform(0,1) distributions for entry parameters ψ constrained to [0,1], and Cauchy (0, 2.5) distributions for detection parameter intercepts μ_t on the logit scale (Gelman et al. 2008). The coefficient parameter describing the effect of overlap, δ, was given a diffuse Student-t(0, 2.5, df = 5) (Gelman et al. 2008).

For each model, we ran 3 chains with different sets of initial values to sample the posterior distributions of parameters of interest. For each chain, the first 10 000 MCMC iterations were discarded after having checked that convergence was satisfactory (referred to as the 'burn-in' period). We visually evaluated the convergence of chains to stationary distributions using both sample trace plots as well as the Brooks-Gelman-Rubin diagnostic (Brooks & Gelman 1998), with values close to 1.00 indicating adequate convergence. We then ran chains for an additional 200 000 iterations, for a total of 20 000 MCMC samples used for inference. We assessed support for the inclusion of overlap using a measure of out-of-sample predictive ability, the widely applicable information criterion (WAIC; Watanabe 2010), where a model with a smaller WAIC is judged a better fit.

3. RESULTS

Collectively, survey efforts from 416 d between 1999 and 2022 resulted in a photo-identification data set of 265 distinctive individuals represented by high-quality photographs from sources with effort information that can be translated into yearly encounter histories for use in CR models. The number of distinctive individuals varied by cluster, with 72 individuals identified from Cluster 1, 52 from Cluster 2, 85 from Cluster 3, and 46 from Cluster 4. The telemetry data set included 53 satellite-tagged groups from the 4 social clusters (Cluster 1, n = 27; Cluster 2, n = 5; Cluster 3, n = 16; Cluster 4, n = 5), ranging from 12 to 199 d of data (mean = 62.5; median = 48.8 d) that were analyzed for population-level space use (Fig. 2).

We fit the pseudospatial and conventional Jolly-Seber model to the 265 individual encounter histories over the 24 yr period and found strong support for the pseudospatial model formulation (ΔWAIC = 28.6). The most recent abundance estimate is 139 individuals (95% CRI = [124, 161]) in 2022 (Table 1). The posterior distribution of the parameter describing the effect of overlap on detection probability was distinctly positive (posterior mean = 0.64, 95% CRI = [0.41, 0.88]), indicating that years with higher survey overlap with cluster-level space use had higher detection probabilities (Fig. 4). Our analysis found that the proportion of distinctive individuals appears to slightly decline across the time series, from roughly 75% of the individuals in encountered groups designated as distinctive in early years to about 70% in 2022 (Table 1, Fig. 3).

We found a negative trend in the abundance estimates with time (posterior mean slope = −1.31 animals yr^{-1}; Fig. 5), though the 95% CRI of the posterior distribution of this derived parameter spanned 0 (95% CRI = [−2.92, 0.141]; Fig. 6). The posterior distribution indicates that there is a 78.6% probability that the trend is negative over the entire time series, though the relationship between abundance estimates and time does not appear linear (Fig. 5). We also report the

Table 1. Number of observed individuals, estimated proportion of distinct individuals ($\hat{\theta}$, estimated using a generalized additive model), and derived abundance by year ($N_{total,t}$, estimated from the pseudospatial Jolly-Seber model) for each year in the study. Values in brackets represent the 95% credible intervals (CRI)

Year	No. of ind.	$N_{total,t}$ [95% CRI]	$\hat{\theta}$ [95% CRI]
1999	20	175 [147, 204]	0.76 [0.65, 0.84]
2000	21	184 [160, 210]	0.75 [0.66, 0.83]
2001	19	185 [162, 210]	0.75 [0.66, 0.82]
2002	5	187 [163, 215]	0.75 [0.67, 0.81]
2003	24	182 [160, 205]	0.74 [0.67, 0.79]
2004	44	192 [174, 212]	0.74 [0.67, 0.80]
2005	30	189 [175, 206]	0.73 [0.68, 0.78]
2006	22	191 [178, 206]	0.73 [0.68, 0.77]
2007	17	193 [181, 209]	0.72 [0.68, 0.77]
2008	60	197 [181, 219]	0.72 [0.67, 0.76]
2009	63	197 [174, 219]	0.71 [0.67, 0.75]
2010	97	201 [184, 219]	0.71 [0.66, 0.75]
2011	68	191 [173, 209]	0.71 [0.65, 0.75]
2012	24	184 [167, 204]	0.70 [0.65, 0.75]
2013	26	174 [157, 194]	0.70 [0.65, 0.75]
2014	42	171 [153, 193]	0.70 [0.65, 0.75]
2015	43	171 [154, 191]	0.70 [0.65, 0.75]
2016	39	163 [145, 184]	0.70 [0.65, 0.75]
2017	72	192 [157, 194]	0.70 [0.65, 0.75]
2018	42	157 [142, 178]	0.70 [0.66, 0.75]
2019	57	152 [137, 172]	0.70 [0.65, 0.75]
2020	50	138 [123, 159]	0.71 [0.65, 0.76]
2021	49	138 [119, 163]	0.71 [0.64, 0.77]
2022	63	139 [124, 161]	0.71 [0.63, 0.78]

Fig. 4. Overlap of survey efforts and social cluster-level space use of the main Hawaiian Islands insular population of false killer whales from 1999 to 2022, calculated using Bhattacharyya's affinity

trend for the last 10 yr of abundance estimates (2013–2022), which is distinctly negative (posterior mean = −5.68 animals per year, 95% CRI = [−8.99, −2.14]; Fig. 6), with a 98.9% probability that the trend is negative over the 10 yr period. The mean annual percent change was −1.09 (95% CRI = [−2.11, −0.023]) over the entire time series and −3.51 (95% CRI = [−5.08, −1.88]) from 2013 to 2022. The decline in abundance across the entire time series is consistent among candidate models (conventional CR model trend mean slope = −1.19, 95% CRI = [−9.86, 2.03]).

3.1. Cluster-level results

From our simulations (see below), it was clear that the full population model as formulated would not suffice for estimating true cluster-level abundances. Instead, we ran the model separately for each cluster. Many parameters were inestimable for Clusters 2 and 4, which have more sparse data, resulting in poor convergence of MCMC chains. Clusters 1, 3, and 4, which make up the most encountered groups in the data set, have similar estimated trends as the full population (Table 2). Cluster 2 is the only cluster with an estimated increasing trend, but the estimated abundances in this model had poor convergence (> 1.1).

3.2. Simulation results

We found that the performance of the pseudospatial model is only marginally compromised by variable tag durations, population trends, and cluster-level abundances (Table 3). Models fit to data with variable tag durations estimated accurate abundance and trends in 3% fewer of the simulated data sets than models with data simulated with constant tag durations. When fit to data generated with variable population trends, we find that the pseudospatial model can better estimate population size and trend than a conventional model, whether the population is growing, shrinking, or remaining constant. While the pseudospatial model still performs well under variable cluster-level abundances, with 90% of fits including an accurate estimate of true abundance, accurate trend detection was less frequent at only 69%. Further-

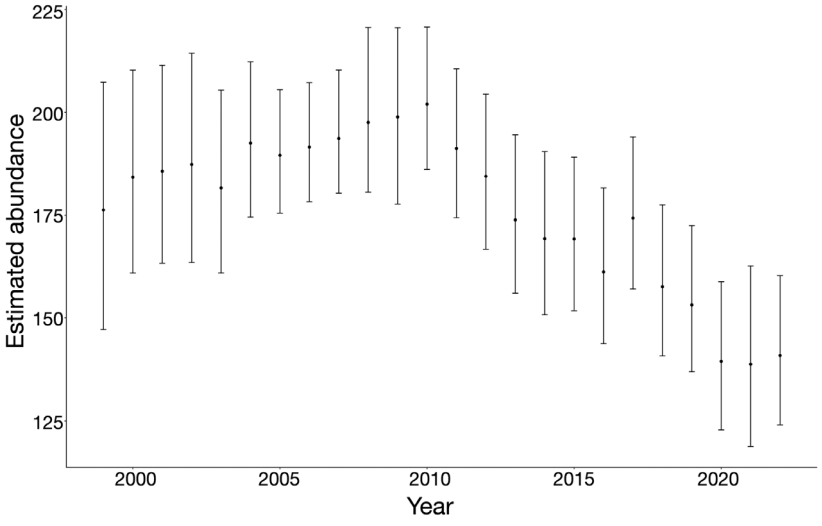

Fig. 5. Abundance of main Hawaiian Islands insular false killer whales, 1999–2022, estimated using a pseudospatial Jolly-Seber model. Dots: posterior mean; error bars: 95% credible intervals

more, upon post-processing calculation of cluster-specific abundances, we found that the model did not accurately estimate the number of individuals in each cluster. As the total population size was still accurate, this is likely linked to cluster 'label-switching' within MCMC chains (Jasra et al. 2005).

4. DISCUSSION

We estimated abundance for the MHI insular population of false killer whales using a pseudospatial model that accounts for animal availability in detection and found the population appears to have declined since it was listed as endangered in 2013 (Fig. 5). Clusters 1 and 3, the most represented clusters in the data set, exhibited similar trends in abundance (Table 2). These results constitute the first robust trend estimates for this population.

We note a decline in the proportion of distinctive individuals throughout the time series, from roughly 75% of the individuals in encountered groups designated as distinctive in early years to about 70% in 2022 (Fig. 4). We suspect that this trend is an artifact of sampling limitations rather than a true decline. Advancements in camera technology have allowed field photographers to have greater group coverage and higher quality photos of all individuals. In early years, film was the primary medium for photographs, and photographers

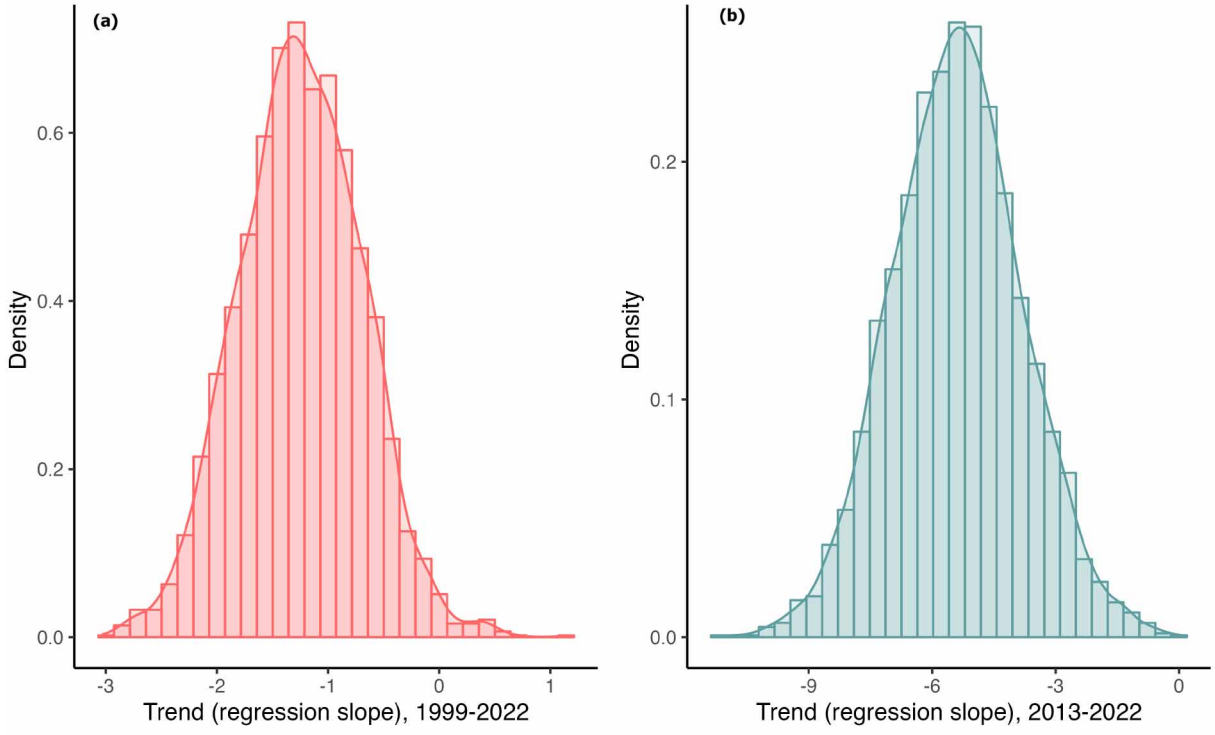

Fig. 6. Posterior distributions of estimated population trends for the entire main Hawaiian Islands insular population of false killer whales from (a) the entire time series, 1999–2022 and (b) the last 10 years of the study, 2013–2022. Trend was estimated as the slope parameter of a regression model fit to the abundance estimates over time and reflects the annual change in the number of individuals in the population

Table 2. Main Hawaiian Islands insular false killer whale cluster-level posterior mean abundance trends estimated using the pseudospatial Jolly-Seber model. Probability of decline over time series is calculated from the posterior distribution of the slope parameter. Values are given as posterior mean [95% credible interval]

Cluster	Trend (entire time series)	Trend (2012–2022)	Mean annual % change (entire time series)	Mean annual % change (2012–2022)	Probability decline of over time series
1	−1.84 [−3.42, −0.037]	−2.93 [−4.01, −1.65]	−1.48 [−0.93, 0.028]	−5.82 [−7.29, −3.22]	0.911
2	1.951 [−0.265, 3.87]	0.36 [−1.99, 1.29]	646 [−10.33, 4200.1]	0.039 [−1.77, 2.08]	0.038
3	−0.352 [−1.393, 0.533]	−1.47 [−2.20, −0.605]	0.14 [−2.38, 0.25]	−1.7 [−5.02, 0.044]	0.655
4	−2.64 [−6.17, 1.26]	−1.82 [−3.62, 0.51]	16.66 [−73.7, 56.95]	−4.4 [−9.2, 0.44]	0.946

Table 3. Performance of the pseudospatial (PS) and conventional (C) Jolly-Seber open population model fit to 30 data sets under 8 different conditions noted (240 data sets total). % true *N* and % with true trend refer to the accuracy (90% credible interval) of posterior distributions of abundance and the slope parameter in a regression fit to yearly abundance estimates. The change in posterior precision was measured as the ratio of posterior standard deviations between 2 competing models

Simulated condition	Model	% True *N*	% True trend	Change in posterior precision
Variable tag duration	PS	87	71	–
Constant tag duration	PS	90	74	1.01
Decreasing trend	C	82	58	–
Decreasing trend	PS	85	62	1.18
Increasing trend	C	80	58	–
Increasing trend	PS	86	64	1.19
Variable cluster abundances	PS	90	69	–
Constant cluster abundances	PS	92	75	1.03

were limited to 36 frames before having to change rolls, limiting the number of photos taken of each individual. The switch to digital cameras in the early 2000s removed this limitation, and as digital camera technology improved, the higher resolution increased the likelihood of high-quality photos being obtained of all individuals. Thus, capturing quality identification photographs of small, fast-moving, and generally nondistinctive individuals increased later in the time series. If the proportion of distinctive individuals in the first portion of the time series is biased high as a result, this may account for the coinciding increasing trend in abundance for those years (1999–2002). If left unaccounted for, this apparent decrease in the proportion of identifiable individuals over time would dampen the estimated magnitude of the population decline. It is possible that there has been a shift in the age structure in the population, with an increase in younger cohorts (less distinctive individuals) coincident with a decrease in older cohorts (more distinctive individuals), given that individuals acquire markings as they age (Baird et al. 2008). However, the relatively low recruitment of individuals into the distinctive (marked) population in recent years (R. W. Baird & S. D. Mahaffy unpubl. data) suggests that this is unlikely.

Analyses of simulated data sets, both in this abundance analysis and in a previous analysis of a shorter time series (Badger et al. 2024), show that using the pseudospatial method will yield higher accuracy and precision in estimating abundance and trend than conventional models. These analyses also showed that the model's performance is relatively unaffected by varying population trends, poor characterization of cluster-level space use, low detectability, and unequal cluster abundances and tag deployment duration. These simulations were designed to target specific sample size considerations in this data set. First, there is a vast disparity in telemetry sample sizes among clusters, such that space use for Clusters 2 and 4 are informed by only 5 tagged false killer whale groups each (after accounting for pseudoreplication among tagged pairs), whereas Clusters 1 and 3 are informed by 27 and 16 tagged groups, respectively. Not only did this sparsity inhibit our ability to adequately characterize cluster-level space use for Clusters 2 and 4 but it precluded us from estimating time-specific space use kernels and thus limited us to assume constant space use over time. Fortunately, simulations indicate that if this limitation mischaracterizes space use, it does not reduce the quality of the abundance estimates to less than that of the conventional CR model (Badger et al. 2024). Our model did estimate a positive effect of overlap on detection probabilities, indicating that our calculated overlap variable is at the very least not random with respect to observed encounter rates and

likely explains some variability in availability. Clusters 2 and 4 are also underrepresented in the visual sighting data, affecting our ability to estimate a cluster-specific trend. Given that Clusters 2 and 4 are generally a small portion of the data regardless of sampling site, it may be that these social clusters have a smaller population size than Clusters 1 and 3. Our simulation exercise indicates that this discrepancy in cluster abundance will not greatly impact estimation of the full population abundance. Regardless, these findings do highlight the need for targeted field efforts in the known ranges of Clusters 2 and 4 (Baird et al. 2023) to better understand how cluster-level dynamics scale up to the population-level decline.

The estimated decline in abundance is consistent among candidate models. Bradford et al. (2018) did not find a similar trend when fitting a conventional CR model to most of the same photo-identification data from 2000 to 2015. While some may argue this is an artifact of the modeling process and not reflective of a true decline in abundance, there is more evidence that the difference stems from the information in the additional data collected since 2015 as well as additional data from prior to 2016 that were not available to Bradford et al. (2018). Badger et al. (2024) fit the pseudospatial model framework to the same data as Bradford et al. (2018), including the sightings data from 2000–2015 from one source (CRC, though the primary results in Bradford et al. 2018 include data from multiple sources) and also did not find a substantial trend in abundance estimates. Further, we fit the pseudospatial model to the full time series of data contributed by CRC from 1999 to 2022, which is the largest portion of the data set with the best-described effort information, and found a similar decline with that data partition. While it garners confidence that the decline is apparent across data partitions and modeling frameworks, the pseudospatial model provides more reliable estimates that have accounted for sampling bias and is better suited to estimate the magnitude of this decline.

Among the known threats to this population of false killer whales, interactions with fisheries have the capacity to cause immediate impacts to the population's viability, as they can inflict injuries that impede survival or can be fatal. False killer whales in Hawaiian waters have been documented depredating catch in nearshore fisheries since the 1960s (Pryor 1975, Shallenberger 1981). There are a variety of both commercial and recreational hook and line fisheries around the MHI, and the target catch of these fisheries largely overlaps with the diet of false killer whales (Baird et al. 2021). There are no observer programs in any of these nearshore fisheries, and strandings of false killer whales are extremely rare (Baird 2016), so evidence of interactions (e.g. hookings) is indirect and limited. False killer whales that ingest hooks or are hooked in the mouth and struggle against gear may acquire injuries to the mouthline or dorsal fin that can be detected from photos taken during encounters (Baird et al. 2015, Harnish et al. 2024). Analyses of photographs over the same period as our abundance and trend analyses reveal that over one-quarter of individuals from this population have evidence of surviving prior fisheries interactions (Harnish et al. 2024). While this method does not allow for an assessment of bycatch directly, it does reveal that depredation of bait or catch is widespread among the population and that hooking occurs regularly. Hook ingestion may lead to mortality or decreased health and longevity for those that do survive (Wells et al. 2008). Furthermore, the Harnish et al. (2024) analysis noted that the proportion of individuals with such fishery-related injuries appeared to vary by cluster, from 19.4% (Cluster 2) to 38.2% (Cluster 4), although this effect was not statistically significant. It is possible that cluster-specific differences in the rates of fishery interactions could contribute to the differences in population trend for each cluster.

Other factors could also be playing a role, including reduced energy intake due to a reduction in prey size or availability, as well as possibly individuals being deliberately killed (Baird 2009, Oleson et al. 2010). While there is no direct evidence for intentional killing of false killer whales in Hawaiian waters, shooting of other species of odontocetes that are at least occasionally involved in fishery interactions has been documented (Kuljis 1981, Tummons 1997, Harnish et al. 2019). Other identified threats to the viability of the MHI insular false killer whale population include exposure to pollutants and reduced genetic diversity (Oleson et al. 2010). Of 56 individual biopsy samples, all adult males and about 1/3 of adult females in the population have levels of PCBs in the blubber that exceed a threshold that could cause impaired reproduction or immunosuppression, where sex-related variation in levels is due to maternal offloading of pollutants to offspring (Kratofil et al. 2020). Analyses of mating patterns have indicated that between 36 and 64% of matings occur within clusters, with the strong social structure further limiting genetic diversity in this small population (Martien et al. 2019). The synergistic effects of 2 or more of these threats could have a strong impact on an endangered population. The loss of a single individual in such a long-lived species can have a meaningful, immediate effect on the dynamics of the population (Williams & Lusseau 2006). As a

highly social, group-living species with significant maternal investment (Mahaffy et al. 2023), false killer whales may also be less resilient to such exploitation; knowledge and leadership by older individuals and cooperative behaviors (e.g. hunting, possible alloparental care) are key for survival and reproductive success (Wade et al. 2012).

This analysis could be improved in several ways for uture abundance estimation. Firstly, the spatiotemporal nature of the data-generating process could be more explicitly defined and incorporated into the modeling framework. Current development of a continuous-time, spatially explicit CR model incorporating a time inhomogeneous Markov-modulated Poisson process could address this point (Choquet 2018, Rushing 2023). Additionally, as we were only able to estimate a static cluster-level space use layer for availability using the telemetry data, further information on temporal variation in animal availability to survey efforts would improve our method. For example, passive acoustic monitoring data could be easily incorporated into this framework, although these data are currently limited to providing presence-only information in small areas over long time periods or broader regions over shorter time scales. However, while false killer whales can be distinguished acoustically from other species (Baumann-Pickering et al. 2015), it is not currently possible to attribute an acoustic detection to a specific population (Barkley et al. 2019). There is some overlap between the MHI insular false killer whales and nearby populations (Baird et al. 2013, Fader et al. 2021, Oleson et al. 2023); thus, incorporating passive acoustic monitoring data would need to take into account the potential for overlap among populations. Incorporating additional auxiliary data into abundance estimation will greatly aid recovery metric accuracy and power to detect trends, as well as stakeholder confidence in management actions for this population.

Data archive. Code and summarized data (encounter histories, utilization distributions) that can be used to run a pseudospatial analysis can be found at https://github.com/badgerjj/pseudospatialCR. The raw data from which these data were made belong to CRC and are subject to their data access requirements.

Acknowledgements. Data used in this analysis was part of a long-term study made possible by multiple grants and contracts from NOAA Fisheries and the US Navy (Living Marine Resources, Office of Naval Research, and Pacific Fleet) to CRC, as well as support from the Tides Foundation, the Marine Mammal Commission, and by the Wild Whale Research Foundation. A myriad of team members, both staff and volunteers, contributed to CRC's long-term odontocete research, and we would like to particularly thank Annie Gorgone for early contributions to CRC's false killer whale catalog. Field research by PWF was funded by members of the PWF and a number of private donors. Photos were collected under NMFS permits 774-1437, 774-1714, and 14097 (issued to SWFSC), 20311 and 15420 (issued to PIFSC), and 20605 (issued to CRC), and under NMFS Scientific Research Permits 926, 731-1509, 731-1774, and 15330 issued to CRC, as well as GA21, 468-1574, LOC13427, 16479, LOC18101, and 21321 issued to PWF. M.A.K. was partially supported by NSF GRFP Award no. 1840998. We thank Erik Franklin and Mark Miller for previous discussions that informed this analysis, as well as anonymous reviewers and Tim Tinker for their technical and editorial insights that greatly improved the manuscript. We also thank Ākeamakamae Kiyuna for the Hawaiian language translation of the abstract.

LITERATURE CITED

Anderson D, Baird RW, Bradford AL, Oleson EM (2020) Is it all about the haul? Pelagic false killer whale interactions with longline fisheries in the central North Pacific. Fish Res 230:105665

Andrews RD, Pitman RL, Ballance LT (2008) Satellite tracking reveals distinct movement patterns for Type B and Type C killer whales in the southern Ross Sea, Antarctica. Polar Biol 31:1461–1468

Bachman MJ, Keller JM, West KL, Jensen BA (2014) Persistent organic pollutant concentrations in blubber of 16 species of cetaceans stranded in the Pacific Islands from 1997 through 2011. Sci Total Environ 488-489:115–123

Badger JJ, Johnson DS, Baird RW, Bradford AL, Kratofil MA, Mahaffy SD, Oleson EM (2024) Incorporating telemetry information into capture–recapture analyses improves precision and accuracy of abundance estimates given spatiotemporally biased recapture effort. Methods Ecol Evol 15:1847–1858

Baird RW (2009) A review of false killer whales in Hawaiian waters: biology, status, and risk factors. Technical Report E40475499. US Marine Mammal Commission, Bethesda, MD

Baird RW (2016) The lives of Hawai'i's dolphins and whales: natural history and conservation. University of Hawai'i Press, Honolulu, HI

Baird RW (2018) False killer whales. In: Würsig B, Thewissen JGM, Kovacs K (eds) Encyclopedia of marine mammals, 3rd edn. Elsevier, London, p 347–349

Baird RW, Gorgone AM, McSweeney DJ, Webster DL and others (2008) False killer whales (*Pseudorca crassidens*) around the main Hawaiian Islands: long-term site fidelity, inter-island movements, and association patterns. Mar Mamm Sci 24:591–612

Baird RW, Schorr GS, Webster DL, McSweeney DJ, Hanson MB, Andrews RD (2010) Movements and habitat use of satellite-tagged false killer whales around the main Hawaiian Islands. Endang Species Res 10:107–121

Baird RW, Hanson MB, Schorr GS, Webster DL and others (2012) Range and primary habitats of Hawaiian insular false killer whales: informing determination of critical habitat. Endang Species Res 18:47–61

Baird RW, Webster DL, Aschettino JM, Schorr GS, McSweeney DJ (2013) Odontocete cetaceans around the main Hawaiian Islands: habitat use and relative abundance from small-boat sighting surveys. Aquat Mamm 39:253–269

Baird RW, Mahaffy SD, Gorgone AM, Cullins T and others

(2015) False killer whales and fisheries interactions in Hawaiian waters: evidence for sex bias and variation among populations and social groups. Mar Mamm Sci 31:579–590

Baird RW, Anderson DB, Kratofil MA, Webster DL (2021) Bringing the right fishermen to the table: indices of overlap between endangered false killer whales and nearshore fisheries in Hawai' i. Biol Conserv 255:108975

Baird RW, Cornforth CJ, Mahaffy SD, Lerma JK, Harnish AE, Kratofil MA (2023) Field studies and analyses from 2020 through 2022 to support the cooperative conservation and long-term management of main Hawaiian Islands insular false killer whales. Report to the State of Hawai'i Board of Land and Natural Resources under Contract No. 68819

Baird RW, Mahaffy SD, Hancock-Hanser B, Cullins T and others (2024) Long-term strategies for studying rare species: results and lessons from a multi-species study of odontocetes around the main Hawaiian Islands. Pac Conserv Biol 30:PC23027

Barkley Y, Oleson EM, Oswald JN, Franklin EC (2019) Whistle classification of sympatric false killer whale populations in Hawaiian waters yields low accuracy rates. Front Mar Sci 6:645

Baumann-Pickering S, Simonis AE, Oleson EM, Baird RW, Roch MA, Wiggins SM (2015) False killer whale and short-finned pilot whale acoustic identification. Endang Species Res 28:97–105

Bradford AL, Forney KA, Oleson EM, Barlow J (2014) Accounting for subgroup structure in line-transect abundance estimates of false killer whales (*Pseudorca crassidens*) in Hawaiian waters. PLOS ONE 9:e90464

Bradford AL, Oleson EM, Baird RW, Boggs CH, Forney KA, Young NC (2015) Revised stock boundaries for false killer whales (*Pseudorca crassidens*) in Hawaiian waters. NOAA Tech Memo NOAA-TM-NMFS-PIFSC-47

Bradford AL, Baird RW, Mahaffy SD, Gorgone AM and others (2018) Abundance estimates for management of endangered false killer whales in the main Hawaiian Islands. Endang Species Res 36:297–313

Brooks SP, Gelman A (1998) General methods for monitoring convergence of iterative simulations. J Comput Graph Stat 7:434–455

Calenge C (2006) The package 'adehabitat' for the R software: tool for the analysis of space and habitat use by animals. Ecol Modell 197:516–519

Ceballos G, Ehrlich PR (2002) Mammal population losses and the extinction crisis. Science 296:904–907

Chivers SJ, Baird RW, Martien KM, Taylor BL and others (2010) Evidence of genetic differentiation for Hawai'i insular false killer whales (*Pseudorca crassidens*). NOAA Tech Memo NMFS-SWFSC-458

Choquet R (2018) Markov-modulated Poisson processes as a new framework in analysing capture–recapture data. Methods Ecol Evol 9:929–935

Conn PB, Ver Hoef JM, McClintock BT, Johnson DS, Brost B (2022) A GLMM approach for combining multiple relative abundance surfaces. Methods Ecol Evol 13:2236–2247

Douglas DC, Weinzierl RC, Davidson S, Kays R, Wikelski M, Bohrer G (2012) Moderating Argos location errors in animal tracking data. Methods Ecol Evol 3:999–1007

Douglas AB, Alpízar FG, Acevedo-Gutiérrez A, Mahaffy SD and others (2023) False killer whales (*Pseudorca crassidens* Cetacea: Delphinidae) along the Pacific coast of Central America and Mexico: long-term movements, association patterns and assessment of fishery interactions. Rev Biol Trop 71:e57189

Dujon AM, Lindstrom RT, Hays GC (2014) The accuracy of Fastloc-GPS locations and implications for animal tracking. Methods Ecol Evol 5:1162–1169

Duong T (2007) ks: kernel density estimation and kernel discriminant analysis for multivariate data in R. J Stat Softw 21:1–16

Fader JE, Baird RW, Bradford AL, Dunn DC, Forney KA, Read AJ (2021) Patterns of depredation in the Hawai'i deep-set longline fishery informed by fishery and false killer whale behavior. Ecosphere 12:e03682

Ferreira IM, Kasuya T, Marsh H, Best PB (2014) False killer whales (*Pseudorca crassidens*) from Japan and South Africa: differences in growth and reproduction. Mar Mamm Sci 30:64–84

Fleming CH, Fagan WF, Mueller T, Olson KA, Leimgruber P, Calabrese JM (2015) Rigorous home range estimation with movement data: a new autocorrelated kernel density estimator. Ecology 96:1182–1188

Gelman A, Jakulin A, Pittau MG, Su YS (2008) A weakly informative default prior distribution for logistic and other regression models. Ann Appl Stat 2:1360–1383

Gelman A, Carlin JB, Dunson DB, Vehtari A, Rubin DB (2013) Bayesian data analysis, 3rd edn. Chapman and Hall/CRC Press, Boca Raton, FL

Hammond PM, Mizroch SA, Donovan GP (eds) (1990) Individual recognition of cetaceans: use of photo-identification and other techniques to estimate population parameters. Rep Int Whaling Comm Spec Issue 12:1–440

Hammond PS, Francis TB, Heinemann D, Long KJ and others (2021) Estimating the abundance of marine mammal populations. Front Mar Sci 8:735770

Harnish AE, Ault J, Babbitt C, Gulland FM and others (2019) Survival of a common bottlenose dolphin (*Tursiops truncatus*) calf with a presumptive gunshot wound to the head. Aquat Mamm 45:543–548

Harnish AE, Baird RW, Mahaffy SD, Douglas AB and others (2024) False killer whales and fisheries in Hawaiian waters: evidence from mouthline and dorsal fin injuries reveal ongoing and repeated interactions. Endang Species Res 55:273–293

Jasra A, Holmes CC, Stephens DA (2005) Markov chain Monte Carlo methods and the label switching problem in Bayesian mixture modeling. Stat Sci 20:50–67

Johnson DS, London JM, Lea MA, Durban J (2008) Continuous-time correlated random walk model for animal telemetry data. Ecology 89:1208–1215

Jolly GM (1965) Explicit estimates from capture–recapture data with both death and immigration–stochastic model. Biometrika 52:225–248

Kéry M, Schaub M (2012) Bayesian population analysis using WinBUGS: a hierarchical perspective. Academic Press, Boston, MA

Kranstauber B, Cameron A, Weinzerl R, Fountain T, Tilak S, Wikelski M, Kays R (2011) The Movebank data model for animal tracking. Environ Model Softw 26: 834–835

Kratofil MA, Ylitalo GM, Mahaffy SD, West KL, Baird RW (2020) Life history and social structure as drivers of persistent organic pollutant levels and stable isotopes in Hawaiian false killer whales (*Pseudorca crassidens*). Sci Total Environ 733:138880

Kuljis BA (1981) Porpoise/fisheries interactions within the Hawaiian Islands. NOAA Administrative Report NMFS-SWFSC H-83-19C

London JM (2020) pathroutr: an R package for (re-)routing

paths around barriers. (Version v0.1.1-beta). https://doi.org/10.5281/zenodo.4321827
Mahaffy SD, Baird RW, Harnish AE, Cullins T and others (2023) Identifying social clusters of endangered main Hawaiian Islands false killer whales. Endang Species Res 51:249–268
Marsh H, Sinclair DF (1989) Correcting for visibility bias in strip transect aerial surveys of aquatic fauna. J Wildl Manag 53:1017–1024
Martien KK, Chivers SJ, Baird RW, Archer FI and others (2014) Nuclear and mitochondrial patterns of population structure in north Pacific false killer whales (*Pseudorca crassidens*). J Hered 105:611–626
Martien KK, Taylor BL, Chivers SJ, Mahaffy SD, Gorgone AM, Baird RW (2019) Fidelity to natal social groups and mating within and between social groups in an endangered false killer whale population. Endang Species Res 40:219–230
Murphy DD, Weiland PS (2016) Guidance on the use of best available science under the US Endangered Species Act. Environ Manage 58:1–14
Nichols JD, Williams BK (2006) Monitoring for conservation. Trends Ecol Evol 21:668–673
Oleson EM, Boggs CH, Forney KA, Hanson BM and others (2010) Status review of Hawaiian insular false killer whales (*Pseudorca crassidens*) under the Endangered Species Act. NOAA Tech Memo NMFS-PIFSC 22
Oleson EM, Bradford AL, Martien KK (2023) Developing a management area for Hawai'i pelagic false killer whales. NOAA Tech Memo NMFS-PIFSC-150
Palmer C, Baird RW, Webster DL, Edwards AC and others (2017) A preliminary study of the movement patterns of false killer whales (*Pseudorca crassidens*) in coastal and pelagic waters of the Northern Territory, Australia. Mar Freshw Res 68:1726–1733
Pebesma E (2018) Simple features for R: standardized support for spatial vector data. R J 10:439–446
Photopoulou T, Ferreia IM, Best PB, Kasuya T, Marsh H (2017) Evidence for a postreproductive phase in female false killer whales *Pseudorca crassidens.* Front Zool 14:30
Plummer M (2003) JAGS: a program for analysis of Bayesian graphical models using Gibbs sampling In: Hornik K, Leisch F, Zeileis A (eds) Proceedings of the 3rd International Workshop on Distributed Statistical Computing (DSC 2003), 20–22 March 2003, Vienna
Plummer M (2018) rjags: Bayesian graphical models using MCMC. R package version 4-8. https://mcmc-jags.sourceforge.io
Pryor K (1975) Lads before the wind: diary of a dolphin trainer. Sunshine Books, North Bend, WA
R Core Team (2022) R: a language and environment for statistical computing. R Foundation for Statistical Computing, Vienna
Rushing CS (2023) An ecologist's introduction to continuous-time multi-state models for capture–recapture data. J Anim Ecol 92:936–944
Schorr GS, Baird RW, Hanson BM, Webster DL, McSweeney DJ, Andrews RD (2009) Movements of satellite-tagged Blainville's beaked whales off the island of Hawai'i. Endang Species Res 10:203–213
Seber GAF (1965) A note on the multiple-recapture census. Biometrika 52:249–260
Shallenberger EM (1981) The status of Hawaiian cetaceans. Technical Report MMC-77/23. US Marine Mammal Commission, Bethesda, MD
Silva IF, Kaufman GD, Rankin RW, Maldini D (2013) Presence and distribution of Hawaiian false killer whales (*Pseudorca crassidens*) in Maui County waters: a historical perspective. Aquat Mamm 39:409–414
Stacey PJ, Leatherwood S, Baird RW (1994) *Pseudorca crassidens*. Mamm Species 456:1–6
Stack SH, Currie JJ, McCordic JA, Olson GL (2019) Incidence of odontocetes with dorsal fin collapse in Maui Nui, Hawaii. Aquat Mamm 45:257–265
Taylor BL, Martinez M, Gerrodette T, Barlow J, Hrovat YN (2007) Lessons from monitoring trends in abundance of marine mammals. Mar Mamm Sci 23:157–175
Tummons P (1997) Fishery council hears of dolphin deaths, sea turtle slaughter, bird bycatch. Environment Hawai'i 8(6):8–9
Vehtari A, Gelman A, Simpson D, Carpenter B, Burkner PC (2021) Rank-normalization, folding, and localization: an improved (formula presented) for assessing convergence of MCMC (with discussion). Bayesian Anal 16: 667–718
Wade PR, Reeves RR, Mesnick SL (2012) Social and behavioural factors in cetacean responses to overexploitation: Are odontocetes less 'resilient' than mysticetes? J Mar Biol 2012:567276
Watanabe S (2010) Asymptotic equivalence of Bayes cross validation and widely applicable information criterion in singular learning theory. J Mach Learn Res 11: 3571–3594
Wells RS, Allen JB, Hofmann S, Bassos-Hull K and others (2008) Consequences of injuries on survival and reproduction of common bottlenose dolphins (*Tursiops truncatus*) along the west coast of Florida. Mar Mamm Sci 24: 774–794
Williams R, Lusseau D (2006) A killer whale social network is vulnerable to targeted removals. Biol Lett 2:497–500
Wood SN (2011) Fast stable restricted maximum likelihood and marginal likelihood estimation of semiparametric generalized linear models. J R Stat Soc Series B Stat Methodol 73:3–36
Yano KM, Oleson EM, Mccullough JLK, Ballance LT and others (2018) Cetacean and seabird data collected during the winter Hawaiian Islands Cetacean and Ecosystem Assessment Survey (Winter HICEAS), January–March 2020. NOAA Tech Memo NMFS-PIFSC-72
Ylitalo GM, Baird RW, Yanagida GK, Webster DL and others (2009) High levels of persistent organic pollutants measured in blubber of island-associated false killer whales (*Pseudorca crassidens*) around the main Hawaiian Islands. Mar Pollut Bull 58:1932–1937
Yoccoz NG, Nichols JD, Boulinier T (2001) Monitoring of biological diversity in space and time. Trends Ecol Evol 16:446–453
Zaeschmar J, Estrela G (2020) False killer whale *Pseudorca crassidens* (Owen, 1846) In: Hackländer K, Zachos FE (eds) Handbook of the mammals of Europe. Springer International Publishing, Cham, p 1–39
Zaeschmar JR, Dagmar Ferti INV, Dwyer SL, Meissner AM and others (2014) Occurrence of false killer whales (*Pseudorca crassidens*) and their association with common bottlenose dolphins (*Tursiops truncatus*) off northeastern New Zealand. Mar Mamm Sci 30:594–608

Editorial responsibility: Robert Harcourt, Sydney, New South Wales, Australia
Reviewed by: H. Pavanato, M. Authier and 1 anonymous referee
Submitted: August 31, 2024; Accepted: May 21, 2025
Proofs received from author(s): August 6, 2025